EFDA–JET–CP(08)04/01

F. Romanelli, J. Paméla, M.L.Watkins, R. Kamendje, S. Brezinsek, Y. Liang,
X. Litaudon, T. Loarer, D. Moreau, D. Mazon, G. Saibene, F. Sartori,
P.C. de Vries and JET EFDA contributors

Recent Contribution of JET to the ITER Physics

Recent Contribution of JET to the ITER Physics

F. Romanelli, J. Paméla[1], M.L.Watkins[2], R. Kamendje[3], S. Brezinsek[4], Y. Liang[4], X. Litaudon[5], T. Loarer[5], D. Moreau[5], D. Mazon[5], G. Saibene[6], F. Sartori[2], P.C. de Vries[2] and JET EFDA contributors*

JET-EFDA, Culham Science Centre, OX14 3DB, Abingdon, UK

[1]EFDA, Close Suppot Unit – Garching, Boltzmannstr. 2, D-85748 Garching, Germany
[2]EURATOM-UKAEA Fusion Association, Culham Science Centre, Abingdon, Oxon OX14 3DB, UK.
[3]Institut für Theoretische Physik-Computational Physics, Technische Universität Graz, Petersgasse 16, A- 8010 Graz, Austria
[4]Association EURATOM-FZJ, Forschungszentrum Jülich GmbH, Institute of Energy Research IEF-4: Plasma Physics, Partner in the Trilateral Euregio Cluster, 52425 Jülich Germany
[5]Association EURATOM-CEA, DSM-IRFM, CEA Cadarache, 13108 Saint Paul lez Durance, France
[6]Fusion for Energy Joint Undertaking, Josep Pl. 2, Torres Diagonal Litoral B3, 08019, Barcelona, Spain
** See annex of M.L. Watkins et al, "Overview of JET Results ", (Proc. 21 st IAEA Fusion Energy Conference, Chengdu, China (2006)).*

Preprint of Paper to be submitted for publication in Proceedings of the 25th Symposium on Fusion Technology, Rostock, Germany (15th September 2008 - 19th September 2008)

ABSTRACT.
In recent years the JET scientific programme has focussed on addressing physics issues essential for the consolidation of design choices and the efficient exploitation of ITER in parallel to qualifying ITER operating scenarios and developing advanced control tools. Active methods have been developed to mitigate, without adversely affecting confinement, edge localised modes (ELMs) along with a systematic characterisation of the edge plasma, pedestal energy and ELMs, and their impact on plasma facing components as well as their compatibility with material limits. The unique JET capability of varying the Toroidal Field (TF) ripple from its normal low value $\delta_{BT} = 0.08\%$ up to $\delta_{BT} = 1\%$ has been used to elucidate the role of TF ripple on confinement and ELMs. Increased TF ripple in ELMy H-mode plasmas is found to have a detrimental effect on plasma stored energy and density, especially at low collisionality. The development of ITER advanced tokamak scenarios has been pursued. In particular, β_N values above the†'no-wall limit' ($\beta_N \sim 3.0$) have been sustained for a resistive time. Gas balance studies combined with shot-resolved measurements from deposition monitors and divertor spectroscopy have confirmed the strong role of fuel co-deposition with carbon in the retention mechanism through long-range migration and also provided further evidence for the important role of ELMs in the material migration process within the JET inner divertor leg.

1. INTRODUCTION

The Joint European Torus (JET) has made unique contributions to the physics basis of ITER [1, 2] by virtue of its ITER-like geometry (non-circular plasma cross-section, single null divertor), large plasma current and Deuterium-Tritium (D-T) capability [3, 4].

In the recent years, the JET scientific programme has focussed on addressing specific issues essential for the consolidation of the design choices and the efficient exploitation of ITER in parallel to qualifying ITER operating scenarios and developing advanced control tools. This paper reviews the recent JET contributions on:

- the control, mitigation and avoidance of Edge Localized Modes (ELMs) that pose a threat to the lifetime of ITER plasma facing components;
- the determination of the maximum toroidal field ripple that can be tolerated on ITER;
- the investigation of carbon migration and tritium retention mechanisms with carbon Plasma Facing Components (PFCs), in preparation of the test with full metal PFCs (beryllium main wall and tungsten divertor);
- the development of scenarios for a steady-state DEMO to be tested in ITER.

These studies have taken advantage of a number of enhanced JET capabilities (see ref. [5] for more details) such as new or upgraded diagnostics and a modified divertor allowing high triangularity ITER-relevant scenarios to be run at high plasma current.

With regard to ELMs, investigations have concentrated on developing active methods to mitigate ELMs without adversely affecting confinement. These methods include resonant magnetic field

perturbation (using Error Field Correction Coils), rapid variation of the radial field (using the vertical stabilisation controller) and ELM pacing using shallow injection of ice pellets.

With regard to the effect of Toroidal Field (TF) ripple on confinement and ELMs, studies have focussed on the use of the unique JET capability of varying the TF ripple from its normal low value $\delta_{BT} = 0.08\%$ up to $\delta_{BT} = 1\%$.

As far as tritium retention is concerned, the JET contribution includes results from gas balance studies performed to provide insights into the retention mechanism and sufficiently characterise fuel retention in an all carbon machine, which is related to the erosion of the primary carbon source (main chamber).

With regard to the demonstration of steady-state tokamak operation at high fusion gain, major progress in operation at high power and/or high β_N values in configurations relevant to ITER steady-state condition has been made at JET.

In the following the physics progress that has been made on JET over the last few years in each of the aforementioned areas is discussed.

2. TYPE-I EDGE LOCALISED MODES AND THEIR MITIGATION IN JET

The foreseen baseline operating scenario for ITER is the Type-I ELMy H mode [6]. This plasma scenario has been widely studied in several tokamak devices and the extrapolation of its confinement properties toward ITER will allow operation at a fusion gain (ratio of fusion power to input power) of $Q_{DT} = 10$ due to the existence of an edge transport barrier. On one hand, the increase of temperature and density gradients at the plasma edge (pedestal formation) leads to a substantial gain in stored energy and fusion performance, but on the other hand, the pressure gradient reaches a critical limit above which so-called Type-I ELMs become unstable. ELMs lead to a periodic expulsion of a considerable fraction of the thermal energy stored in the plasma onto the PFCs. Although ELMs may be beneficial in controlling the particle inventory and removing impurities and helium ashes, the associated transient loads on PFCs are unacceptable in ITER. Extrapolation based on present machines indicates that the transient heat loads in ITER will probably be such to lead to erosion/ melting with a reduction in PFCs lifetime [7] to unpractical levels. Although not discussed in the present paper, a further problem that already arises in present tokamaks and that will be crucial in ITER is that the coupling of radio frequency heating power to the plasma becomes poor in the presence of large ELMs. In this regard, in 2008 JET has started testing an ITER-like ion cyclotron resonance heating antenna that features ELM tolerance [8]. The aim of this antenna is to demonstrate power coupling at ITER-relevant power density and plasma conditions using a close-packed array of straps mounted as four Resonant Double Loops, each consisting of two poloidally adjacent straps, arranged in a 2 toroidal by 2 poloidal array. ELM tolerance is incorporated using an internal (in-vacuum) conjugate-T junction with each strap fed through in-vessel matching capacitors from a common vacuum transmission line. Recent experiments have shown that by tailoring the plasma shape and adjusting the gas injection, H-mode regimes with small ELMs [9] can be accessed on

smaller machines. However, on larger machines such as JET, this is only possible over a limited range of plasma parameters [10]. Therefore, in ITER, active methods are required for the control of ELMs, aiming at reducing the power loading on plasma facing components, without adversely affecting the energy confinement.

The effect of perturbing magnetic fields on the stability of ELMs has been investigated on several tokamaks [11, 12, 13]. In particular, complete suppression of Type-I ELMs has been demonstrated on DIII-D with resonant magnetic fields (n = 3) [14], where n is the toroidal mode number of the perturbation. All the DIII-D experiments were carried out with in-vessel magnetic coils.

2.1 ELM MITIGATION WITH EXTERNAL MAGNETIC PERTURBATION FIELDS

At JET, successful ELM mitigation experiments with External Magnetic Perturbation Fields (EMPFs) induced by the Error Field Correction Coils (EFCCs) mounted outside of the vacuum vessel (see figure 1) were carried out. The toroidal mode number spectrum of the EFFCs system at JET is limited to n = 1 and n = 2 perturbations. The first results from this experiment showed that the frequency and the amplitude of type-I ELMs can be actively controlled by the application of an n = 1 EMPF generated by the EFCCs as described in Ref [15]. During the application of the n = 1 field in ITER-relevant configurations and parameters in a wide operational space of plasma triangularity (upper triangularity δ_U up to 0.45), the ELM frequency increased by a factor of 4. The energy loss per ELM normalized to the total stored energy, $\Delta W/W$, decreased from 7% to below the noise level of the diamagnetic measurement (less than 2%). Such a condition was maintained for a duration of 10 time the energy confinement time. It was also shown that ELM mitigation does not depend on the orientation of the n = 1 external fields and ELM mitigation is achievable in wide range of the edge safety factor, q_{95} (4.8-3.0). The reduction in ELM amplitude, the simultaneous increase in ELM frequency, and a reduction in fast ion losses were observed independent of the phase of the n = 1 field. A reduction in ELM peak heat fluxes (by roughly the same factor as the increase in ELM frequency [16]) on and in carbon erosion (reduced physical sputtering) of the divertor target plates are observed during the ELM mitigation phase. The application of EMPFs leads to a density pump-out whose origin is not fully understood and that must be compensated by increased gas puffing. Nevertheless, transport analysis using the TRANSP code shows at most a modest reduction of the thermal energy confinement time due to the density pump-out and, when normalized to the IPB98(y,2) confinement scaling [1], the confinement shows almost no reduction. Time traces for a typical ELM mitigation experiment are shown in figure 2 [17]. ELM mitigation with the n = 1 field has also been shown in JET to be applicable in high beta plasmas (β_N up to ~3.0 as foreseen in ITER AT scenarios) [18] without causing the degradation of thermal energy confinement time and with the ELM frequency increased by a factor of ~3 and no additional heating power requested to maintain a constant energy content. The first results of ELM mitigation with the n = 2 EMPFs on JET have demonstrated that the ELM frequency can be increased by a factor of 3.5 even with a limited EFCC coil current [17]. A wide operational window of q_{95} has also been obtained for ELM mitigation with n = 2 EMPFs. A strong

braking of the toroidal plasma rotation has been observed during the ELM mitigation with either the n=1 or the n=2 EMPFs, indicating that non-resonance magnetic braking could play a role affecting the plasma rotation. Such a braking is expected due to the low toroidal mode number spectrum produced by the EFCCs that induces magnetic perturbation extending well inside the plasma. A new system of resonant magnetic perturbation for JET is under study in order to overcome this problem and to reproduce a spectrum similar to that produced by the ITER internal coils.

2.2 MAGNETIC ELM PACING USING THE VERTICAL STABILISATION CONTROLLER

At JET, first experimental evidence of the application of a rapid varying radial field as ELM pacing mechanism has been obtained [19]. The JET Vertical Stabilization (VS) controller [20] has been modified to allow the application of a user defined voltage pulse (so called kick) at an adjustable frequency which can be synchronised to the ELM event or applied asynchronously. The periodic pulse generation is implemented by introducing a count-down timer in the VS. When the counter reaches zero, the desired voltage pattern is generated and sent to the amplifier. If this mechanism is synchronised then the counter is restarted at every occurrence of an ELM, as detected by a rapid variation on one of the divertor D_α traces. With this technique the kicks are only applied if the natural ELM-free period is larger then the timer setting. In addition, this means that the kick is never applied just after a naturally occurring ELM thus compounding the disturbance to the VS system. Initial results [19] achieved on deuterium target plasmas with a low density H-mode and low frequency Type-I ELMs (single null magnetic configuration, $I_p = 1.9$MA, $B_t = 2.35$T, $q_{95} = 3.7$, elongation k = 1.72) show that it has been possible to increase the natural ELM frequency by at least a factor of 5 and to moderate the initial large ELM (figure 3) while keeping the baseline plasma stored energy unchanged (figure 4). Work is presently ongoing at JET to further develop this method and accurately document the effects of the kicks on the edge transport barrier, the ELM structure and the changes in ELM power loadings on the divertor and first wall.

2.3 ELM PACING USING SHALLOW INJECTION OF ICE PELLETS

ELM triggering by pellet injection provides a promising method for reducing the ELM size as demonstrated on ASDEX Upgrade [21]. However, ELM pacing in this way should be achieved with the smallest possible impact on all other plasma parameters (besides ELM frequency). Hence, pellet injection for ELM pacing should use the smallest possible pellets and a shallow injection. In 2007 JET has installed a new High Frequency Ice Pellet Injector (HFPI) [5] that is currently being commissioned for experiments. The design parameters of the HFPI are such that, for ELM pacing purposes, it should be able to inject an unlimited number of pellets (variable pellet volume 1–2mm^3, pellet speed 50–200m/s and frequency up to 60Hz) with a very high level of reliability. A successful scaling to ITER from ELM pacing results from present day tokamaks requires a mature physics understanding. To this end, besides demonstrating ELM pacing with the new HFPI, detailed investigations of the local impact of the pellet-imposed perturbation will be carried out at JET.

2.4 MITIGATION OF ELM-INDUCED POWER LOADS BY IMPURITY SEEDING

An alternative way to achieve a substantial reduction of the power load to the target plates during ELMs is the use of extrinsic impurities to increase or replace the intrinsic radiation. This usually leads to a transition to the highly radiating Type-III ELMy H-mode regime. At JET substantial progress has been achieved in extending this regime with N_2 seeding to higher plasma currents up to 3MA and, hence, higher densities (up to 1.1×10^{20} m^{-3}) [22]. The advantage of this plasma regime is the tolerable ELM size in perspective of ITER, even though at slightly reduced confinement (~10-15%) as compared to the reference H-mode regime. This scenario could extrapolate to Q_{DT} = 10 in ITER at 17MA and density approaching the Greenwal density limit ($n_{GW} = I_p/(\pi a^2)$, with the increased current compensating for the loss of confinement (confinement enhancement factor over the IPB98(y,2) scaling [1] $H_{98}(y,2)$=0.75) induced by impurity injection.

3. TOROIDAL FIELD RIPPLE EFFECTS ON H-MODES IN JET AND IMPLICATIONS FOR ITER

In all tokamak devices, the finite number and toroidal extension of the toroidal magnetic field coils causes a periodic variation of the TF from its nominal value, called the TF ripple defined as $\delta_{BT} = (B_{max}-B_{min})/(B_{max}+B_{min})$. Standard operations at JET are carried out with a set of 32 TF coils all carrying equal current. However, uniquely to JET, it is possible to vary the TF ripple amplitude by independently powering the 16 odd and 16 even numbered coils. The imbalance current between the two coil sets can be changed in a controlled way, thereby increasing the TF ripple from its nominal value at the separatrix (outboard mid-plane) δ_{BT} ~ 0.08% up to δ_{BT} ~ 3%. It is well known that ripple in the toroidal field adversely affects fast ion confinement and, in the case of ITER, this has been accounted for by including in the design Ferritic Insets (FI) compensation, aiming at reducing δ_{BT} from ~1.2% down to ~0.5% (at full field) [23]. Previous experimental results from JT60-U [24] and dimensionless H-mode experiments in JET and JT-60U [25] had indicated that ripple may also affect the H-mode confinement and plasma rotation. Although the physics mechanisms at the root of the reduced energy confinement with δ_{BT} was not identified unambiguously, the implication of a reduction of energy confinement on projected ITER performance due to ripple stimulated a series of experiments at JET aiming at quantifying, for a range of plasma conditions, the impact of ripple on confinement and attempting to identify an acceptable maximum ripple for ITER. In these experiments, the effect of ripple on H-mode was investigated by first establishing an H-mode reference discharge with Type I ELMs at δ_{BT} of 0.08% and then increasing the ripple in steps (0.3%, 0.5% and 0.7%) from pulse to pulse to a maximum of 1%. The average TF was set at B_t (toroidal magnetic field) =2.2T and 1.7T. Most studies were carried out at plasma current I_p = 2.6MA / B_t = 2.2T (q_{95} ~ 2.9, safety factor at 95% of the poloidal flux), in a low triangularity plasma shape (δ ~ 0.22). In all cases, additional heating was provided by Neutral Beam (NB) co-current injection.

3.1 BEHAVIOUR OF PLASMA CONFINEMENT, PEDESTAL AND ROTATION WITH RIPPLE

The results of the experiments can be summarised as follows. Increasing the toroidal field ripple in plasmas with no gas fuelling in the H-mode phase has a detrimental effect on plasma density (figure 5) and confinement (figure 6), especially at low pedestal collisionality [26]. Specifically, increasing δ_{BT} from the standard 0.08% level to 1% causes a reduction of the confinement enhancement factor, $H_{98}(y,2)$, of ~20% with most of the density loss already observed at δ_{BT} = 0.5%. Within the measurement uncertainty, the deterioration of plasma confinement with ripple magnitude is continuous (although not necessarily linearly proportional to δ_{BT}). The very non-linear dependence of Q_{DT} on the confinement enhancement factor $H_{98}(y,2)$ ($\sim H_{98}(y,2)^{3.3}$) implies that even "small" reductions of the plasma confinement would result in a reduction of the fusion power not acceptable for ITER. The effect of the reduction of both the average and the pedestal density in the H-mode phase (density "pump-out", ~ 30% loss for δ_{BT} = 0.5% and >40% loss for δ_{BT} = 1% as compared to the reference H-mode discharge) associated with increasing ripple needs careful consideration for the projected ITER Q_{DT} = 10 plasma conditions. In fact, the fusion power output is proportional to the density (at constant normalised pressure β). Therefore, the impact of density pump out on Q_{DT} is even more severe than what is deduced from the reduction of the $H_{98}(y,2)$ factor.

The effect of external gas fuelling was investigated by adding increasing amounts of gas to the reference plasmas described above. Although the most striking effect of ripple is the strong density pump out, the plasma response to external gas fuelling is similar, independent of the ripple value. At the highest fuelling rates the difference between an H-mode with 0.08% and 1% ripple becomes very small in terms of achievable density, edge temperature and energy confinement [26].

As already shown in figure 5, even for small TF ripple amplitudes of δ_{BT}~0.5% the JET plasma rotation is significantly reduced compared to normal levels. In the discharges with δ_{BT} ~0.5% a counter current torque was found in the order of 20-30% of that supplied by the NBI system in co-current direction [27]. For a series of dedicated ELMy H-mode discharges, besides showing a decrease of the dimensionless thermal Mach number (= ratio of rotation velocity and thermal velocity) and total angular momentum with δ_{BT}, figure 7 also shows that for δ_{BT}~1% an area of counter rotation develops at the edge of the plasma, while the core keeps its co-rotation. The dominant mechanism that drives the observed counter rotation in the discharges with a large δ_{BT}>0.5% can be associated with banana orbit diffusion of trapped energetic ions (by NBI). However, calculations with the ASCOT code of the induced torque due to these losses do not fully explain the observations. The edge rotation in the presence of a large TF ripple appeared to depend on the local ion temperature, suggesting that other ion losses, possibly those of thermal ions, may be involved. The effect of TF ripple on thermal ions has so far not been included in the ASCOT calculations. Predictions for plasma rotation in ITER often assume that the momentum and energy confinement times are proportional and do not include TF ripple effects [28]. However, as shown in the bottom part of figure 7 for the JET discharges, the momentum confinement time (defined as the ratio of the total

angular momentum and the applied torque by NBI) is found to be much smaller than that of the energy confinement time, while for standard TF ripple (δ_{BT} = 0.08%) these two parameters are found to be of the same order of magnitude. The values of momentum confinement time calculated using the torque as calculated by ASCOT, which include the effects of TF ripple on energetic ions, are shown in figure 7 to be larger than the original confinement times but still drop with ripple amplitude and are considerably lower than those of the energy confinement. Therefore, predicting plasma rotation in ITER by extrapolating from present devices, like JET, which have significantly lower TF ripple may be more complicated. The TF ripple induced torque is always in counter current direction and will reduce the NBI co-current torque, yielding a lower rotation in ITER than presently expected.

Another important issue associated with the TF ripple is its effect on the formation and strength of Internal Transport Barriers (ITB) essential for the viability of AT scenarios on ITER. Dedicated experiments have shown that, although the ITB trigger was unaffected (figure 8), the further development of the ITB may be degraded due to larger TF ripple [29]. The TF ripple reduces the toroidal rotation and modifies the toroidal rotation profile (figure 9) while no effect on the poloidal rotation has been observed. It suggests that stronger barriers form in the presence of a larger rotational shear. The ITB triggering was unaffected by the changes in rotational shear and, in these experiments, this mechanism may be predominantly determined by the detailed shape of the safety factor profile.

3.2 Effect of TF ripple on Edge Localised Modes

The analysis of the JET data shows that toroidal field ripple affects ELM frequency and size [26] as illustrated in figure 10. With increased ripple from 0.08% to 0.5% the type I ELM frequency almost doubles, going from ~12Hz to ~20Hz. With ripple increased further to 0.7% and finally 1%, ELMs become irregular, with Type I, Type III and long ELM-free phases, in spite of the fact that power across the separatrix remains approximately constant. Moreover, the data indicate that Type I ELM size is reduced, for 1% ripple, by about a factor of two and that the ELM losses seem to become more convective. Although a reduction of the ELM size may look attractive for ITER, the JET results show that this would come at the price of significant confinement deterioration. Therefore, the JET results suggests that δ_{BT}<0.5% is required in ITER in order to achieve the Q_{DT} = 10 goal and reduce the uncertainty on confinement extrapolation as well as the impact on plasma rotation.

4. FUEL RETENTION STUDIES

In ITER, without any cleaning effort, a retention of 10% of the Tritium (T) injected (T injection rate ~5×10^{22}T s^{-1}) during the 400s of burning phase would lead to the limit of 700g of mobilisable T (nuclear licensing) within only 100 discharges. Thus the evaluation of fuel retention in present tokamaks is of high priority to establish a database for ITER, for which gas balance will be the dominant technique used to assess the fuel retention. The overall particle balance has been studied in JET in a series of repetitive and identical discharges with an overall accuracy of about 1.2%. The particle retention behaviour has been analysed [30] for L-modes and H-modes (Type III and Type

I ELMs) discharges in the same magnetic configuration with the following parameters: plasma current I_p = 2MA, magnetic field B_T = 2.4T, average particle density $\langle n_e \rangle = 4.5\times10^{19}m^{-3}$, gas injection rate 1.8×10^{22} Ds^{-1} with 10+3MW of NBI and ICRH, respectively, for the Type I ELMy H-mode, 5.5MW of ICRH only for the Type III ELM experiments and 1.5MW of ICRH only for the L-mode experiments. For all the experiments, active pumping was ensured by the divertor cryopump only (all main chamber pumps closed) and its regeneration (to liquid nitrogen temperature) before and after the series (~at least 1/2 hour after the last pulse) thus allowing a direct measure of the long term retention. The two basic mechanisms for long term fuel retention are the deep implantation (through diffusion or migration in the bulk material) and the co-deposition of hydrogenic species (hydrogen, deuterium, tritium) with carbon and/or berylium. In JET (and also in other carbon devices) co-deposition has been found to dominate the long term retention and it is also expected to be the case for Beryllium within the future ITER-like wall in JET [31] and in ITER. The overall results for the three different scenarios investigated in JET are summarised in table 1 [30]. The short term (dynamic) retention is found to be important for both L mode and Type III ELMy H-mode over the heating phases (respectively 13 and 17sec) but decreases already significantly during the shot. It becomes small already after 6sec for the Type I ELMy H-mode conditions. In all the cases, the recovery after the pulse contributes for a weak part in the gas balance and in the overall fuel retention. When averaged over the heating phase, the long term fuel retention (associated with co-deposition) is ~$2.04\times10^{21}Ds^{-1}$ for the L-mode, ~$2.40\times10^{21}Ds^{-1}$ for the Type III ELMy H-mode and $2.83\times10^{21}Ds^{-1}$ for the Type-I ELMy H-mode. These values are in reasonable agreement with the value deduced from post mortem tile analysis of about $5\times10^{20}Ds^{-1}$, considering that this value from post mortem analysis is an average over the full experimental campaign which includes various plasma parameters (average heating power of only ~4MW [30]) and configurations and also wall conditioning and disruptions. The increase of the long term retention observed from L mode to Type-I ELMy H-mode is associated to the increase of the recycling flux and the carbon flux resulting from erosion in the main chamber. The larger long term retention is attributed to an enhanced carbon erosion and transport in the scrape-off layer, leading to stronger carbon deposition and fuel co-deposition. These results confirm the strong concerns about fuel retention in a carbon clad tokamak and indicate that full carbon in all PFCs in ITER is not viable. A reasonable ITER operation time thus depends on a significant reduced T co-deposition under different material conditions and on effective routine T removal techniques (which have to be confirmed in a relevant tokamak experiment such as the JET ITER-like Wall project [31]). For its low activation phase, ITER is currently designed to have an all-beryllium-clad first wall, tungsten brushes over most of the divertor region and carbon fibre composites only at the target plates where the highest power fluxes are expected (divertor strike points). For the high activation phase ITER is planned to have an all-tungsten divertor.

Besides fuel retention, the physical mechanisms underlying material erosion, long and short range migration and re-deposition within the present full carbon walls in JET have been addressed

with the particular aim to prepare for future comparisons with results from the foreseen ITER-like wall. These studies have benefited from improved diagnostics and dedicated pulse sequences. Spatial distribution and layer characteristics have been identified with dedicated slow plasma sweeps and spatially resolved hydrocarbon spectroscopy and Quartz microbalance deposition detectors which have been placed around the JET divertor. The main results can be summarised as follows [32]:

(i) Carbon is mainly released from first wall and deposited in the inner divertor. The magnetic configuration is the main factor which determines the deposition pattern in first place, e.g. the private flux region turns from net deposition to erosion when the configuration changes from vertical to horizontal target operation.

(ii) The deposited carbon undergoes further transport inside the divertor by a stepwise process induced by new magnetic configurations which lead to enhanced re- erosion of freshly deposited layers. This erosion is much stronger than for bulk graphite substrate.

(iii) This effect is partly attributed to the disintegration of deposited layers by plasma impact far before normal carbon sublimation sets in. Spectroscopy shows that this is accompanied by thermal decomposition of a-CH layers and possible release of carbon clusters.

(iv) A strongly nonlinear increase of the local carbon release and migration inside the divertor with ELM size has been found such that a few large type I ELMs lead to a stronger migration than many small ELMs [33].

These observations can explain the large carbon deposition and tritium retention on remote areas (louvers) in the JET DTE1 experiments in 1997. They show also that the dynamics of carbon transport is a specific carbon property related to the chemical sputtering probability, which is then coupled with the deposition and fast disintegration of carbon layers. Such effects are not expected for metallic layers such as beryllium that will be use in the main chamber of ITER. At JET beryllium evaporation is applied to condition the first wall, to getter oxygen with a protective layer and reduce the hydrocarbon content. However, the beryllium conditioning typically lasts only for a small number of discharges and carbon is still the predominant impurity in the plasma. Dedicated first wall erosion studies with fresh beryllium evaporated wall have been recently performed [34] demonstrating that the beryllium layer in the main chamber is eroded in a similar way as carbon and beryllium is transported to the inner divertor leg. However, the main difference to carbon is the fact that beryllium remains close to the location of the inner strike-point. This view is also supported by the fact that the beryllium content in layers on plasma facing areas in the inner divertor reaches values of typically 20% while carbon layers in remote areas are strongly de-enriched from their beryllium content by factors in between 10-100.

5. PROGRESS IN ADVANCED TOKAMAK SCENARIOS

In a tokamak, a plasma scenario is defined as the sequence of operational events applied to prepare and then initiate the plasma, raise the plasma current to the required value, apply the auxiliary

heating during the burning phase and finally extinguish the plasma discharge safely. The tokamak uses a transformer such that the secondary current (the plasma current) is driven inductively by continuously increasing the current in the primary circuit. This feature effectively limits the pulse length to the time for the poloidal field coils to reach their maximum achievable currents. For this reason, in ITER, the baseline plasma scenario (ELMy H-mode) is envisaged to operate for a duration not exceeding 500s at a plasma current of 15MA. The optimization of the inductive tokamak concept for steady-state regime is referred to as "advanced tokamak" (AT) research. The objective of the AT research is to provide a candidate plasma scenario for continuous operation in a fusion power plant such as DEMO [35]. In ITER, fully non-inductive operation (i.e. without transformer flux consumption) is envisaged for up to 3000s with Q_{DT}~5 and a bootstrap current fraction f_{BS} (= I_{boot}/I_P) typically above 50% at a normalized beta of the order of $\leq_N$~2.9 [36] and a reduced plasma current I_P = 9MA, corresponding to q_{95}~5. To compensate for the reduction in energy confinement associated with reducing the plasma current (needed to minimise the current that must be driven by external power sources), the ITER steady-state regime must achieve improved confinement as compared with the ELMy H-mode scaling. An improvement factor of $H_{IPB98(y,2)}$~1.5 is required simultaneously with a high absolute density ($n \sim 6.5\times10^{19} m^{-3}$) corresponding in turn to a high density normalized to the Greenwald density, n_l/n_{Gw}~0.8 where $n_{GW} = I_P/(\pi a^2)$. Achievement of higher confinement relies on the combination of an edge transport barrier (as obtained in H-mode) with an ITB as reviewed in Ref. [37, 38]. The fraction of the plasma current driven by the bootstrap mechanism scales as: $f_{BS} \sim C_{BS}\beta_N q_{95}$, with the normalised pressure $\beta_N = \beta_t(\%)a(m)B_T(T)/I_p(MA)$ where $\leq_t$ is the plasma pressure normalized to the toroidal magnetic field pressure in percentage; a is the minor radius in metre; B_T is the on-axis toroidal magnetic field in Tesla and I_p is in megampere. C_{BS} is a parameter depending weakly on current and pressure profile parameters. Therefore, the achievement of high bootstrap current fraction relies on operation at high β_N values,†typically above the usual values imposed by the MHD no-wall limit [39]. In addition, fusion performance optimization in steady-state should be obtained in conditions compatible with the ITER Plasma-Facing Components (PFCs). This requires operation at high edge density to achieve plasma steady-state and transient edge conditions compatible with high radiation levels and reduced peak heat load on divertor tiles. AT operation at simultaneous high confinement and high β_N is challenging since it requires the use of highly shaped plasmas and active control of the pressure and current density profiles to operate close to or, even, above the standard tokamak operational limits, together with active control of the radiated power fraction. At present, the approach at JET consists of addressing these various critical issues separately with a view to full scenario integration when the JET upgrades [5] are complete. The progress achieved so far is summarised in the following [40, 35, 41].

5.1 ITER-like shape and high density operation

Regimes with ITBs have been developed at q_{95}~5 and high triangularity, δ ~0.5 (relevant to the ITER steady-state demonstration) by applying up to 30MW of additional heating power reaching

β_N ~2 at B_T~3.1T, I_p~1.9MA (see figure 11). For these discharges at high triangularity, the improved confinement factor $H_{98}(y,2)$ does not exceed 1.1 since either: (i) the edge confinement has the characteristics of the standard Type-I ELM regime without improved core confinement; or (ii) the edge pedestal is degraded (e.g. in the Type-III ELM regimes with gas puffing) and the improved core confinement serves to compensate for the degradation of the edge transport barrier. Regimes at high triangularity naturally provide access to high density operation compared with standard low triangularity configurations, allowing the edge pedestal and core densities to be increased pushing the ion temperature closer to that of the electrons. As shown in figure 12, access to higher density at the top of the pedestal is a possible route for the development of high core density plasmas where the density normalized to the Greenwald density has reached n_l/n_{GW}~0.8 at β_N~2.5, approaching simultaneously the values envisaged for ITER.

5.2 HIGH β_N OPERATION WITH ITB AND REAL TIME PROFILE CONTROL

High β_N (up to ~2.8 at B_T~2.3T, I_p~1.5MA) regimes with improved confinement through the generation of ITBs in the ion heat channel at mid-radius with up to 30MW of additional heating power [42, 43, 44, 45, 46] and with small amplitude Type-I ELMs or Type-III ELMs [42, 47, 48] have been sustained for eight confinement times (but shorter than the resistive current diffusion time). The limitation in duration is thought to be due to a slow evolution of the current density profile leading to core MHD instabilities. Discharges at reduced field, B_T~1.8T (I_p~1.2 MA), were performed with the objective to sustain plasmas close to or above the no-wall limit to study the conditions for optimizing plasma stability in the case of weak, or even without, improved core confinement. In regimes with good edge confinement and Type-I ELMs, β_N values of ~3.0 (above the no-wall limit) have been sustained for a resistive current diffusion time (~7s) with ~15MW of NBI power [49, 46, 50]. Moreover, the no-wall limit has been experimentally probed by resonant field amplification using the external error field correction coils as a diagnostic [50]. An imposed oscillating (10–20 Hz) error field is created by the coils and the plasma response is recorded during the high β phase of AT scenario experiments. When the pressure exceeds the no-wall limit this imposed error is amplified so that the β value when the plasma becomes unstable can be determined. Ultimately, sustaining very high β_N values on a resistive current diffusion time scale will require real-time active plasma profile control with a higher fraction of non-inductive current, in addition to the control of the global parameters (e.g. β_N control), either using q-profile control alone or in combination with pressure profile control. In this context a major effort has been made at JET to develop an advanced (two-time scale) dynamic-model approach for a magnetic and kinetic profile control scheme that uses, as actuators, the combination of heating and current drive systems in their routine operation mode and, optionally, the poloidal field system, in an optimal way to regulate the evolution of several pressure and current profile parameters [41]. The profile controller is articulated around two composite feedback loops operating on the magnetic and kinetic time scales, respectively, and supplemented by a feedforward compensation of density variations. Note that the integration

of magnetic and kinetic profiles - known to be strongly coupled - into a single controller is particularly relevant to AT scenarios in future fusion devices such as ITER where the heating and current drive actuators will be quite constrained. In order to overcome the issue of the controller being too sensitive to rapid plasma events such as the spontaneous emergence of ITB or MHD instabilities, a technique for the experimental identification of a dynamic plasma model has been developed, taking into account the physical structure and couplings of the transport equations, but making no quantitative assumptions on the transport coefficients or on their dependences [51]. The model identification technique uses singular perturbation methods in order to cope with the high dimensionality of the system and with the small ratio, μ, between the confinement and resistive diffusion time scales. It was shown to yield reduced-order models which could fairly reproduce the slow and the fast evolution of a few profile coefficients, in some broad vicinity of a reference equilibrium plasma state. As an example, the control of the q profile has been performed at high toroidal magnetic field and reduced $\leq_N$ values (B_T~3T, I_p~1.1–1.5MA). Figures 13 and 14 show that the control phase lasted more than 7 s using the three heating and current drive systems (Lower Hybrid, NBI, ICRH) while separately requesting constant loop voltage [41, 52]. The successful experiments made so far demonstrate that an important step has been made towards the development of an integrated magnetic and kinetic control methodology. Future JET experiments should address (i) the control of the safety factor over the entire plasma radius (10 profile coefficients) with three heating and current drive (H&CD) actuators and at constant boundary flux and (ii) the simultaneous control of the current and electron and/or ion temperature profiles in advanced operation scenarios. Using the H&CD systems together with the poloidal field system for controlling (i) the plasma shape, (ii) the magnetic and kinetic plasma profiles and (iii) the boundary flux, could then provide the essential part of an integrated scheme for achieving high performance non-inductively driven advanced tokamak discharges in JET and the technique could be adapted to any tokamak to provide a broad basis for developing integrated profile control and steady-state advanced scenarios in ITER.

5.3 EDGE CONTROL FOR AT OPERATION AND COMPATIBILITY WITH ITER WALL MATERIAL CONDITIONS

Optimising the fusion performance with the constraints imposed by the ITER PFCs is an important issue and challenge that will be addressed on JET to provide timely preparation of the ITER scenarios. Operation with the new ITER-Like Wall (ILW) at high power will set new constraints on non-inductive scenarios that need to be properly identified [40]. The different investigated approaches aiming at developing AT scenarios compatible with the future metallic wall in JET can be summarised as follows [40]:

- Injection of high-Z radiative gas, such as neon, to increase the edge radiation. Two regimes with mild ELM activity have been found at a power radiation fraction either P_{rad}/P_{tot}~30%, with high frequency Type I ELMs, or at $P_{rad}/P_{tot}\geq$50%, with Type III ELMs or an L-mode edge [47]. It is not obvious that the first regime at P_{rad}/P_{tot}~30% could be directly translated

to future experiments with the new ILW since the radiation level is mainly determined by carbon. Regimes at $P_{rad}/P_{tot} \geq 50\%$ usually require higher core confinement to compensate for the reduction of pedestal energy.

- Sweeping of the strike points to spread the heat load on the divertor tiles [53].
- Change of the magnetic configuration. Quasi-double null plasmas are able to reach a grassy ELM regime as defined in Ref. [10]. The mild grassy ELM regime has been combined with core ITB on the ion heat transport channel. However, a grassy ELM regime at q_{95}~5 has not been achieved so far due to the present lack of additional heating power.
- Ergodization of the magnetic field lines at the plasma edge in the high triangularity/high $\leq_N$ scenario at reduced magnetic field [18]. In this case, the reduction in confinement at the edge transport barrier was compensated by an increase of the core energy content.

Despite the fact that progress has been made in terms of optimizing the magnetic configuration, safety factor profile, increasing the plasma density and increasing $\leq_N$, a further major effort is required to increase the thermal energy content and the bootstrap current fraction on JET, in particular in wall-compatible scenarios. A possible route to further increase the core confinement at high density could be to increase the applied heating and current drive power [54]. In this context, the future JET enhancements, which include a power upgrade together with the modification of the PFCs, will provide a unique opportunity to develop wall-compatible scenarios at high fusion performance together with the high bootstrap current fraction required for steady-state.

CONCLUSIONS AND OUTLOOK

In the recent past, JET has taken advantage of its assets such as ITER-like geometry, large plasma size, Beryllium capability and the capability to vary the toroidal field ripple to make several contributions to the understanding of physics issues essential for the efficient exploitation of ITER in parallel to qualifying ITER operating scenarios and developing advanced control tools. The contributions include:

- the control, mitigation and avoidance of ELMs, with in particular the active control of the frequency and the amplitude of Type-I ELMs by the application of an n = 1 external magnetic perturbation field generated by the error field correction coils;
- the determination of the maximum toroidal field ripple of $\delta_{BT}<0.5\%$ that can be tolerated on ITER;
- the investigation of carbon migration and tritium retention mechanisms with carbon Plasma Facing Components (PFCs), in preparation of the test with full metal PFCs (beryllium main wall and tungsten divertor);
- the developments of scenarios for a steady-state DEMO to be tested in ITER.

In the near term, based on the new capabilities following the enhancement programme that is currently underway [5] and will be completed in 2010, JET will be able to make essential contributions to ITER in several fields [55]:

- the qualification of the ITER scenarios (especially the hybrid and steady-state scenarios) at low normalised Larmor radius ρ_* thanks to the increase of the auxiliary power up to 45 MW;
- the consolidation of the ITER design choices, such as those related with the choice of the plasma facing materials, through the test of a Beryllium wall and a Tungsten divertor;
- the development of control tools for ELM control/amelioration via shallow pellet injection, resonant magnetic perturbation, impurity seeding and plasma shape control;
- the test of radio-frequency antennae for optimized wave-plasma coupling under transient conditions;
- the basic understanding of plasma dynamics through a better set of diagnostics and simulation codes.

After the testing of the ITER-like wall, a D-T experiment is envisaged, to allow extrapolation of the scenarios to ITER relevant conditions.

ACKNOWLEDGEMENT

This work has been carried out within the framework of the European Fusion Development Agreement. The views and opinions expressed therein do not necessarily reflect those of the European Commission.

REFERENCES

[1]. ITER Physics Basis, Nucl. Fusion **39** (1999) 2368
[2]. Progress in the ITER Physics Basis, Nucl. Fusion **47** (2007) S1
[3]. JET Team, Nucl. Fusion **41** (2001) 1327
[4]. M. Keilhacker, Plasma Science & Technology **6** (2004) 2109
[5]. J. Paméla, F. Romanelli, M.L. Watkins, A. Lioure, G.F. Matthews, V. Philipps et al., Fusion Engineering and Design **82** (2007) 590
[6]. F. Wagner et al., Phys. Rev. Lett. **49**, (1982)1408.
[7]. A. Loarte et al., J. Nucl. Mater. **313–316** (2003) 962.
[8]. F. Durodie et al., Commissioning on test bed of the ITER-Like ICRF Antenna for JET, this conference
[9]. J. Stober et al., Nucl. Fusion **41**, (2001) 1123
[10]. G. Saibene et al., Nucl. Fusion **45** (2005) 297
[11]. M. Mori et al., Plasma Phys. Control. Fusion **38** (1996) 1189
[12]. S.J. Fielding et al., Proc. 28th EPS Conf. on Plasma Physics (Funchal, Portugal, 2001) vol 25A (ECA) 1825

[13]. T. Evans et al., Phys. Rev. Lett. **92** (2004) 235003
[14]. T. Evans et al., Nature Phys. **2** (2006) 419
[15]. Y. Liang et al., Phys. Rev. Lett. **98** 265004
[16]. S. Jachmich et al. Proc. 34th EPS Conf. on Plasma Phys. Control. Fusion (Warsaw, 2007)
[17]. Y. Liang et al., Plasma Phys. Control. Fusion **49** (2007) B581
[18]. H.R. Koslowski et al., Proc. 34th EPS Conf. on Plasma Phys. Control. Fusion (Warsaw, Poland, 2007) P5.135
[19]. F. Sartori et al., Synchronous ELM Pacing at JET using the Vertical Stabilisation Controller, Proc. 35th EPS Conf. on Plasma Phys. Control. Fusion (Crete, 2008)
[20]. F. Sartori et al., The Joint European Torus, Plasma position and shape control in the world's largest tokamak, IEE Control System Magazine, vol.26 Number 2, April 2006
[21]. P.T. Lang, A. Kallenbach, J. Bucalossi, G.D. Conway, A. Degeling, R. Dux, et al., Nucl. Fusion **45** (2005) 502.
[22]. J. Rapp et al., Highly radiating Type-III ELMy H-mode with low plasma core pollution, Proc. Of the 18th Int. conf. Plasma-Surface Interacttions in Contr. Fusion Devices, 26-28 May 2008, Toledo, Spain
[23]. 2007 ITER Project Integration Document ITER D 2234RH ed J How (Version 3 2007)
[24]. H. Urano et al., IAEA FEC 2006, EX/5-1
[25]. G. Saibene, N. Oyama, J. Lönnroth3, Y. Andrew, E. de la Luna, C. Giroud et al., Nucl. Fusion **47** (2007) 969
[26]. G. Saibene, R. Sartori, P. de Vries, A. Loarte, J. Lönnroth, V. Parail et al., Results of the Variable Toroidal Field Ripple Experiments in JET, to be submitted to Nucl. Fusion (2008)
[27]. P.C. de Vries, A. Salmi, V. Parail, C. Giroux, Y. Andrew, T.M. Biewer et al., Nucl. Fusion 48 (2008) 035007
[28]. A.R. Polevoi et al., 2002 Proc. 19th Int. Conf. on Fusion Energy 2002 (Lyon, France, 2002) (Vienna: IAEA) CD-ROM file CT/P-08
[29]. P.C. de Vries et al., Plasma Phys. Control. Fusion **50** (2008) 065008
[30]. T. Loarer et al., Proc. of the 18th Int. conf. Plasma-Surface Interacttions in Contr. Fusion Devices, 26-28 May 2008, Toledo, Spain
[31]. J. Paméla, G.F. Matthews, V. Philipps, R. Kamendje, J. Nucl. Mater. **363-365** (2007) 1
[32]. S. Brezinsek et al., Material erosion and migration studies in JET and its implications for ITER, submitted to Plasma Phys. Control. Fusion (2008)
[33]. A. Kreter et al., Non-linear Impact of Edge Localized Modes on Carbon Erosion in the Divertor of the JET Tokamak, accepted for publication in Phys. Rev. Lett. (2008)
[34]. K. Krieger et al., Evolution of Be migration after Be evaporation in the JET tokamak, Proc. 34th EPS Conf. on Plasma Phys. Control. Fusion (Warsaw, Poland, 2007)
[35]. E. Joffrin, Plasma Phys. Control. Fusion **49** (2007) B629
[36]. C. Gormezano et al., Fusion Sci. Technol. 53 (2008) 958

[37]. J. Connor et al., Nucl. Fusion 44 (2004) R1
[38]. X. Litaudon, Plasma Phys. Control. Fusion 48 (2006) A1
[39]. Y. Lin-Liu and R. Stambaugh, Nucl. Fusion 44 (2004) 548
[40]. X. Litaudon et al., Plasma Phys. Control. Fusion 49 (2007) B529
[41]. D. Moreau et al., Nucl. Fusion **48** (2008) 106001
[42]. J. Mailloux et al., Development of ITB plasmas at high $\leq_N$ and high triangularity in JET, Proc. 34th EPS Conf. on Plasma Phys. Control. Fusion (Warsaw, 2007) P4-151
[43]. V. Pericoli et al., Proc. 5th IAEA Technical Meeting on Steady State Operations of Magnetic Fusion Devices (Daejeon, Republic of Korea, 2007)
[44]. V. Pericoli et al., High β_N experiments at JET in ITER-like plasmas in support of the ITER steady state scenario, Proc. 35th EPS Conf. on Plasma Phys. Control. Fusion (Crete, 2008)
[45]. R. Cesario et al., Lower hybrid current drive in experiments for transport barriers at high β_N of JET, Proc. 17th Topical Conf. on Radiofrequency Power in Plasmas (Clearwater, FL, May 2007)
[46]. M. P. Gryaznevich et al., Experimental identification of the beta limit in JET, Proc. 34th EPS Conf. on Plasma Phys. Control. Fusion (Warsaw, 2007) P1-070
[47]. M.N.A. Beurskens et al., Nucl. Fusion **48** (2008) 095004
[48]. G. Arnoux et al., Divertor heat load in ITER-like advanced tokamak scenarios on JET. Submitted to J. Nucl. Mater. (2008)
[49]. C.D. Challis et al., High β_N JET H-modes for steady-state application, Proc. 34th EPS Conf. on Plasma Phys. Control. Fusion (Warsaw, 2007) P5-124
[50]. M. P. Gryaznevich et al.,Experimental Studies of Stability and Beta Limit in JET, submitted to Plasma Phys. Control. Fusion 2008
[51]. D. Moreau et al., Proc. 21st Int. Conf. on Fusion Energy 2006 (Chengdu, China) (Vienna: IAEA), CD-ROM file (EX/P1-2) and http://wwwnaweb.iaea.org/napc/physics/ FEC/ FEC2006/html/node57.htm#14844
[52]. D. Mazon et al. Proc. of the International Workshop on Burning Plasma Diagnostics, Villa Monastero,Varenna, Italy. (24th -28 September 2007)
[53]. A. Pironti et al., A new algorithm for strike point-sweeping at JET, Proc. 34th EPS Conf. on Plasma Phys. Control. Fusion (Warsaw, 2007) P5-116
[54]. X. Litaudon et al., Nucl. Fusion **47** (2007) 1285
[55]. F. Romanelli, Fusion Sci. Technol. **53** (2008)1217

Pulse type	Injection rate (Ds^{-1})	Heating phase (s)	Long term retention (Ds^{-1}) (heating phase)	Divertor phase (s)	Long term retention (Ds^{-1}) (divertor phase)
L-mode	~1.8×10^{22}	81	2.04×10^{21}	126	1.27×10^{21}
H-mode Type III	~1.7×10^{22}	72	2.40×10^{21}	126	1.37×10^{21}
H-mode Type I	~1.7×10^{22}	32	2.83×10^{21}	50	1.70×10^{21}

Table 1: Total number of particles injected, recovered from cryopump regeneration and long term retention, averaged over the heating phase, for the three series of experiments in L mode, Type III and Type I ELMy H-mode.

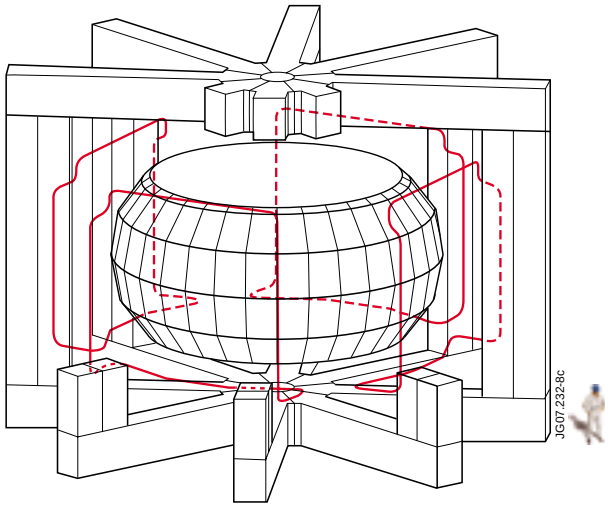

Figure 1: Perspective view of JET showing the four large error field correction coils mounted between the transformer limbs

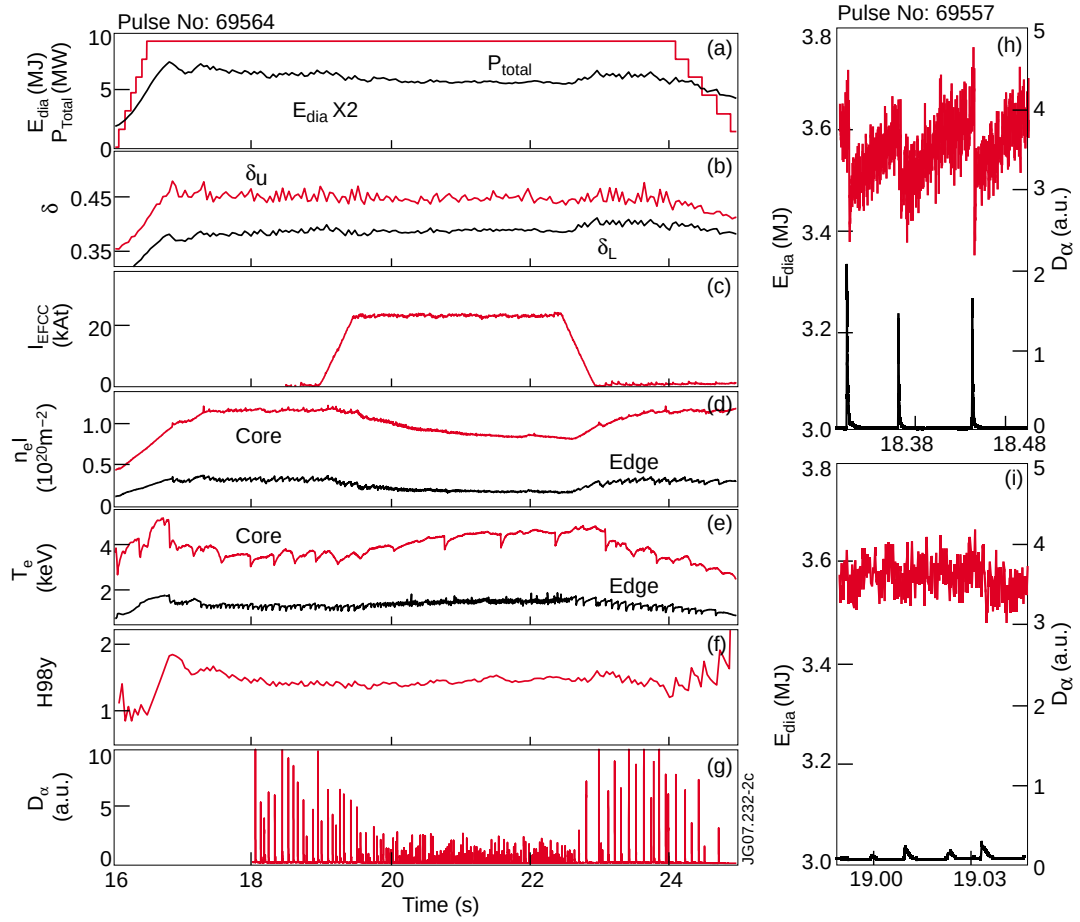

Figure 2: (a-g) Overview of a typical ELM mitigation experiment in a high triangularity plasma on JET. The time traces of the total stored energy, E_{dia}, and the intensity of the $D_{\pm}$ lines measured before (h), and during (i) ELM mitigation with the n = 1 EFCCs are from a discharge similar to the one shown in (a-g).

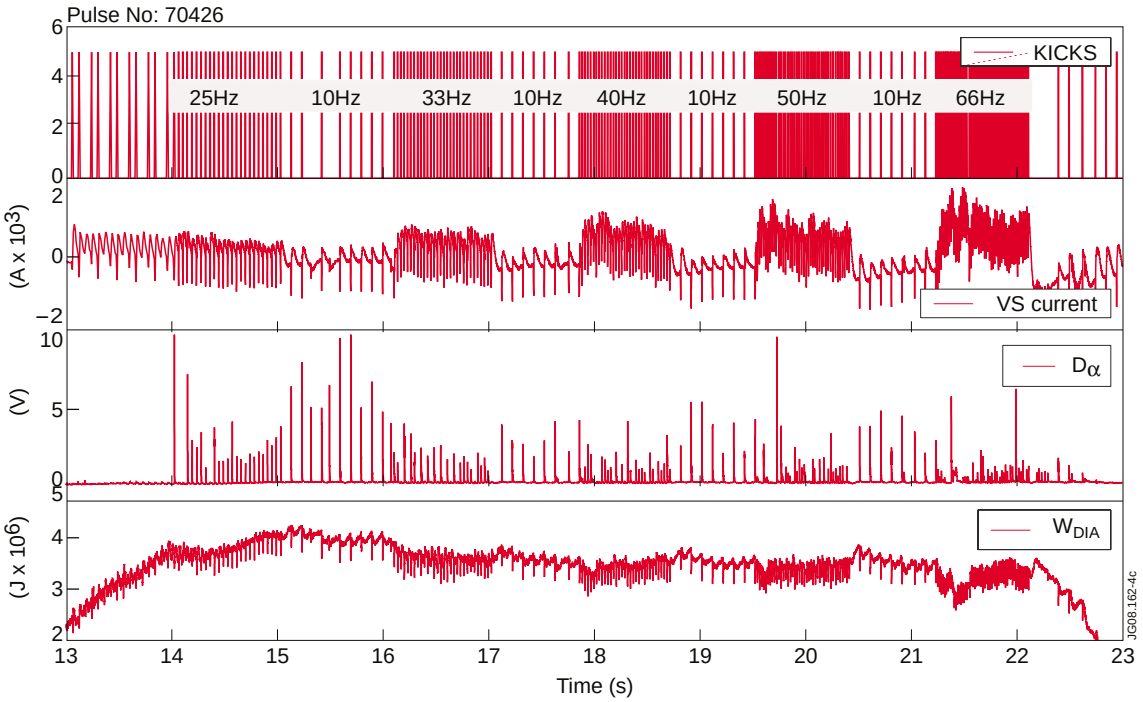

Figure 3: Example of magnetic ELM pacing at JET. The rapid variation of the kick frequency induces an immediate change in ELM frequency (D_α trace), proving that the plasma has no memory of the kick.

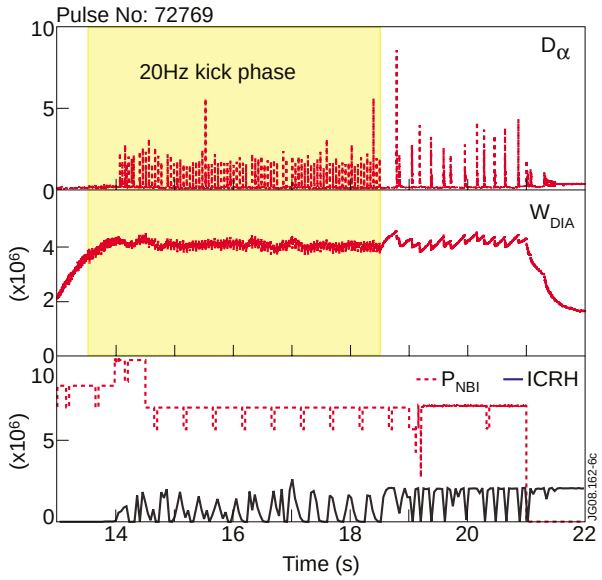

Figure 4: Demonstration that magnetic ELM pacing using vertical kicks to the plasma does not strongly affect the plasma baseline stored energy.

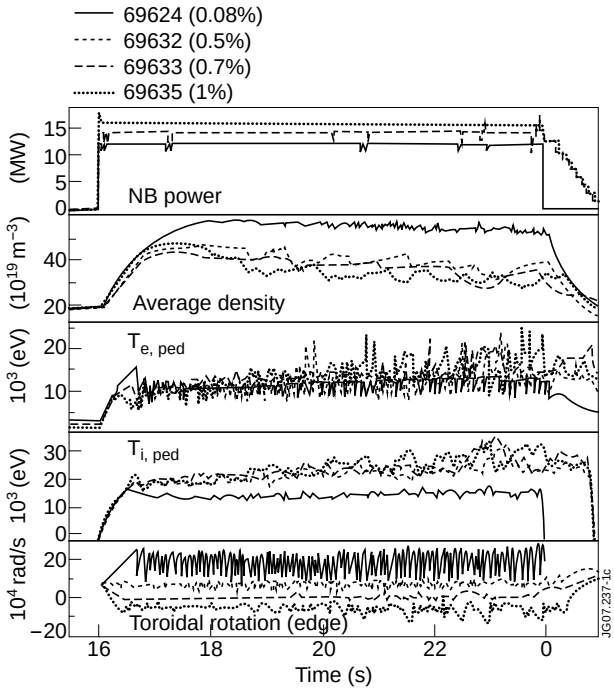

Figure 5: Experimental time traces for a 4-step ripple scan, with no gas fuelling in the H-mode phase (2.6MA/ 2.2T), at constant absorbed power ~ 12.5-13MW (losses are up to 20% of input power). From top to bottom: NB input power, average density, pedestal electron, Te, and ion, Ti, temperature and edge toroidal rotation .

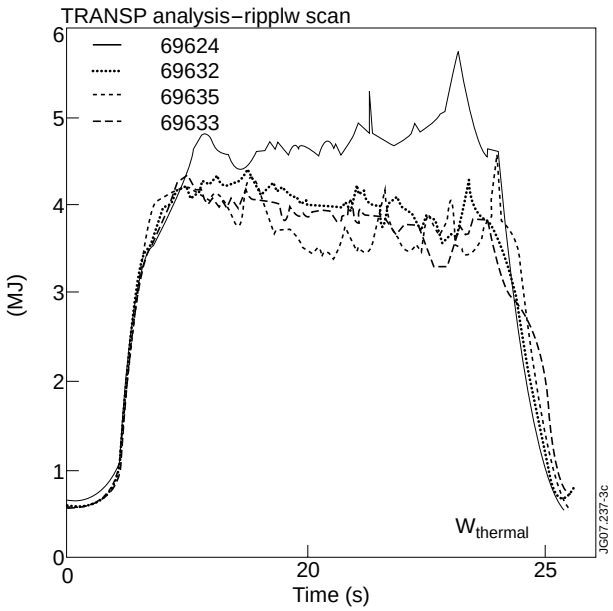

Figure 6: Plasma thermal stored energy, W_{th}, as calculated with TRANSP for the 4-step ripple scan in figure 3. Most of the W_{th} loss is already observed at δ_{BT}=0.5%.

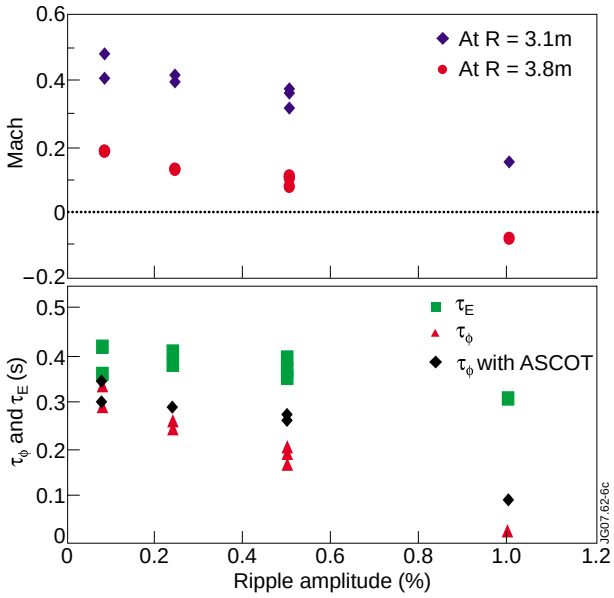

Figure 7: Series of identical type I ELMy H-modes pulse but with increasing TF ripple. The top graph shows the core (R = 3.1m) and edge (R = 3.8m) Mach number, while the bottom graph presents the energy (green squares) and momentum (red triangles) confinement times. The black diamonds show the momentum confinement times with the toroidal torque calculated by ASCOT.

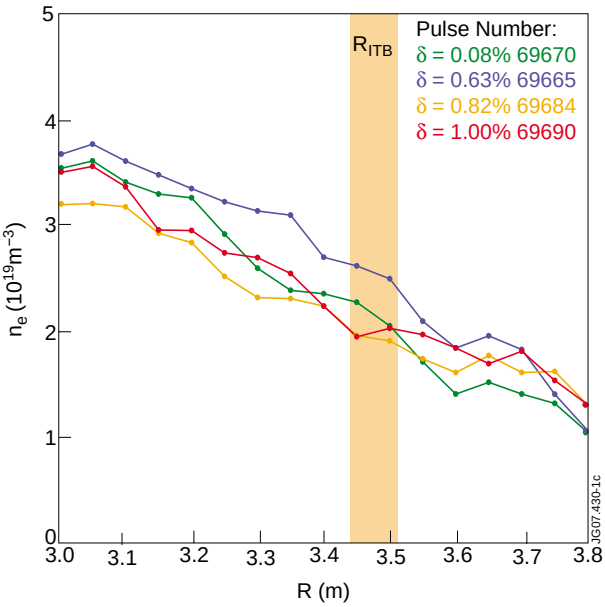

Figure 8 The ion temperature profiles as measured by the CXRS diagnostic for four discharges (reversed shear scenario) with equal absorbed power (P_{abs} = 14.5± 0.2MW) taken at two times: at the time the ITB is triggered (~ t = 4.5s) (dashed lines) and at the time of its maximum strength (solid lines). The centre of the plasma is at R = 3.05m (ρ = 0) and the separatrix at R = 3.85m (ρ = 1)

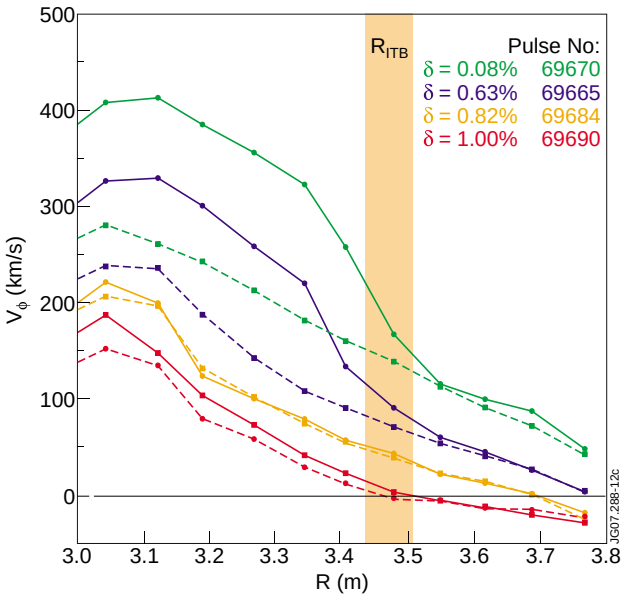

Figure 9: The toroidal rotation profiles (for carbon) as a function of the normalised poloidal flux, ¡, for the four discharges (reversed shear scenario) with equal absorbed power (P_{abs} = 14.5 ± 0.2MW) taken at two times: at the time the ITB is triggered (~ t = 4.5 s) (dashed lines) and at the time of its maximum strength (solid lines). The centre of the plasma is at R = 3.05m (ρ = 0) and the separatrix at R = 3.85m (ρ = 1).

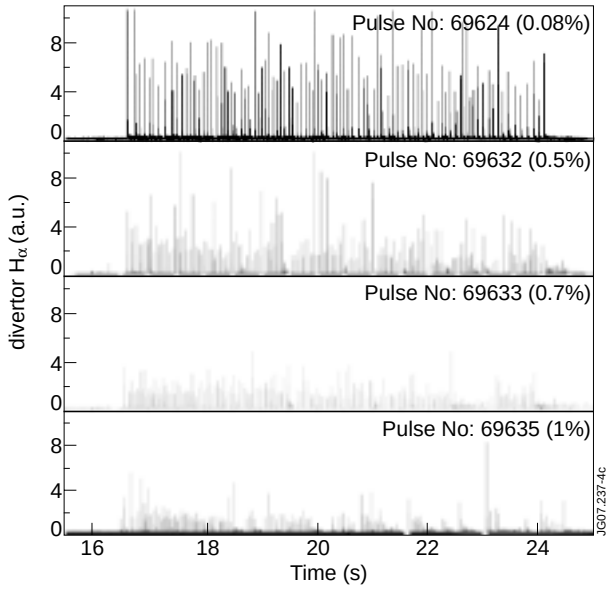

Figure 10:Divertor H-alpha traces for the four plasma discharges in figure 3

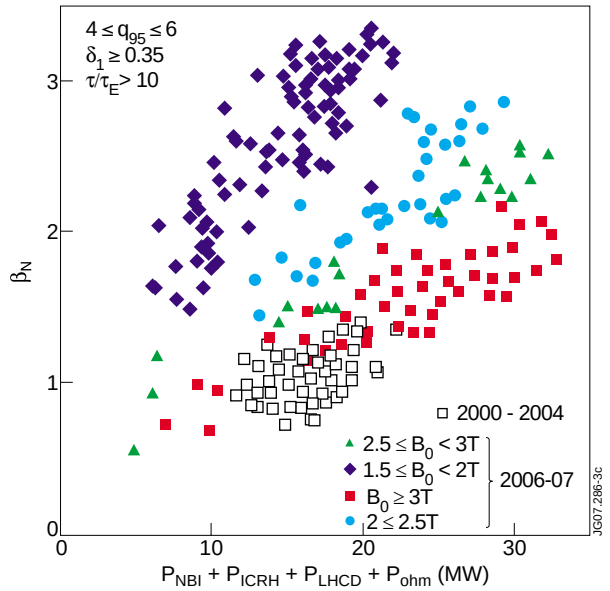

Figure 11: β_N plotted versus the total input power in the main heating phase for various toroidal magnetic fields (each point corresponds to one discharge taken from the 2000–2007 JET-EFDA advanced scenario database). The data are selected at $4 \le q_{95} \le 6$, $\delta_l \ge 0.35$, $\tau/\tau_E > 10$ where f is the duration of high performance phase and τ_E the diamagnetic energy confinement time. ρ_l is the lower trinagularity.

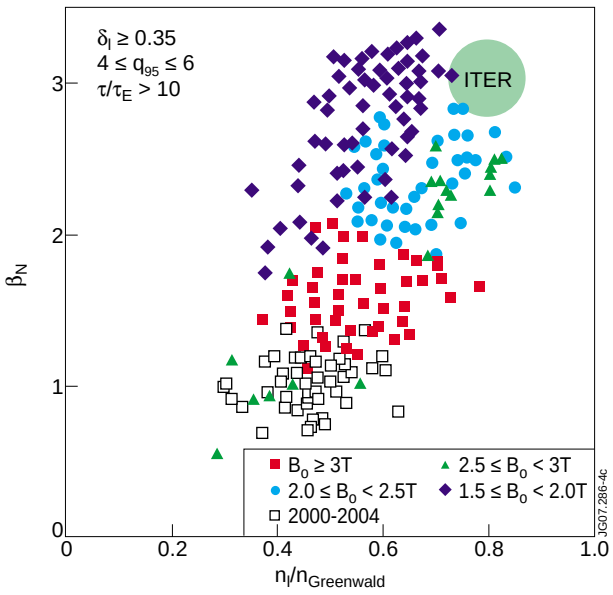

Figure 12: β_N plotted versus the line averaged density normalized to the Greenwald density, n_l/n_{GW} for various toroidal magnetic fields for high triangularity configurations. The data are selected at $4 \le q_{95} \le 6$, $\delta_l \ge 0.35$, $\tau/\tau_E > 10$ as in figure 3. Each point corresponds to one discharge taken from the 2000–2007 JET-EFDA advanced scenario database.

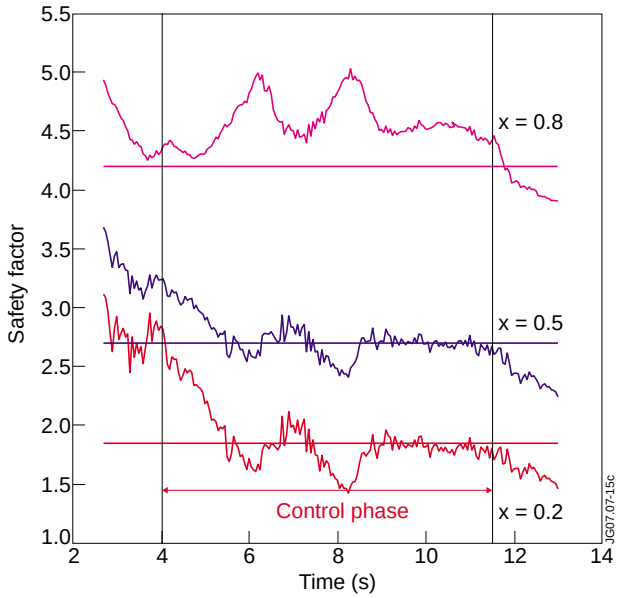

Figure 13 Control of the safety factor profile at three normalized radii, x = 0.2 (red), x = 0.5 (blue) and x = 0.8 (magenta) using the three heating and current drive actuators (Pulse No: 70395). During the control phase the loop voltage is requested constant ($32mV_{rad}^{-1}$). Target values are represented by horizontal lines. The LH system failed to deliver the power requested by the controller (2 instead of 3MW) resulting in a somewhat high value of q at x=0.8 (4.5 instead of 4.2).

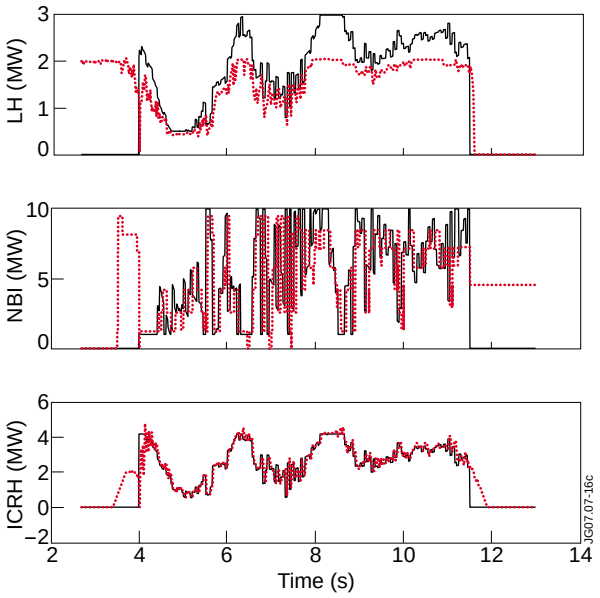

Figure 14: Requested (black traces) and delivered (red dotted traces) LH, NBI and ICRH powers for Pulse No: 70595.